New Journal of Physics
The open-access journal for physics

Michaelis–Menten dynamics of a polymer chain out of a dichotomous ATP-based motor

Alessandro Fiasconaro[1,2,4], **Juan José Mazo**[1,2] **and Fernando Falo**[1,3]

[1] Departamento de Física de la Materia Condensada, Universidad de Zaragoza, C/Pedro Cerbuna, 12 50009 Zaragoza, Spain
[2] Instituto de Ciencia de Materiales de Aragón, CSIC-Universidad de Zaragoza, C/Pedro Cerbuna, 12 50009 Zaragoza, Spain
[3] Instituto de Biocomputación y Física de Sistemas Complejos, Universidad de Zaragoza, C/Pedro Cerbuna, 12 50009 Zaragoza, Spain
E-mail: afiascon@unizar.es

New Journal of Physics **14** (2012) 023004 (12pp)
Received 16 July 2011
Published 2 February 2012
Online at http://www.njp.org/
doi:10.1088/1367-2630/14/2/023004

Abstract. We present a model of an ATP-fueled molecular machine which pushes a polymer through a pore channel. The machine acts between two levels (working–waiting), and the working one remains active for a fixed time giving a constant force. The activation rate of the machine can be put in relationship with the available ATP concentration in the solution, which gives the necessary energy supply. The translocation time shows a monotonic behaviour as a function of the activation frequency, and the velocity follows a Michaelis–Menten (MM) law that arises naturally in this description. The estimation of the stall force of the motor follows a corrected MM law which yet is to be checked in experimental investigations. The results presented here agree with recent biological experimental findings.

[4] Author to whom any correspondence should be addressed.

Contents

1. Introduction

In recent years there has been significant progress in the experimental and theoretical study of transport mechanisms of molecules inside cells and/or through cell membranes [1]. This effort is now attracting more and more attention from researchers in different scientific disciplines. The increasing interest in this subject is related not only to the intrinsic importance of understanding the basic mechanisms of the living systems, but also to the enormous improvement in technological capabilities at the nanometre length scale. These, on the one hand, allow us to detect and measure mechanisms at the nanoscale and, on the other, open up the possibility of constructing from scratch structures (with both natural and synthetic materials) able to imitate biological functioning [2]. In this context, the passage of biomolecules through nanopores is ubiquitous, in both biological and nanotechnological processes. Examples of these two types are the passage of mRNA through nuclear pores [3] and the translocation of DNA in graphene pores [4].

In most cases, translocation is driven by constant fields in the pore or by the difference in chemical potential between the two sides of the membrane. However, in some cases the translocation is assisted by an ATP-based molecular motor [5]. This is the case of DNA bacteriophages in which the incoming DNA has to overcome substantial pressure inside the virus capsid. This makes this kind of motor possibly the most powerful of those known. In this type of motor, ATP hydrolysis fuels the process.

In this paper, we model the translocation process of a one-dimensional (1D) chain pushed by a molecular motor activated by ATP absorption. The motor is able to drive with a constant force a polymer chain in one direction while in its activated state. The polymer diffuses freely otherwise [6, 7]. The work reveals the Michaelis–Menten (MM) behaviour of the polymer velocity and relates it to the MM enzymatic reaction, according to a microscopic reinterpretation of the MM kinetics, which is a very important topic of investigation [8–10].

We will also study the behaviour of the motor against a pulling force, the motor stall force, and its ability to package the polymer in a finite region, as a first approach to a capsid effect.

The aim of this paper is to present a simple model that captures the main physical ingredients of the process. Remarkably, the model is able to well describe some experimentally observed results and make new predictions. The model could also be applied to different kinds of systems. In this spirit, we do not pretend here to give a detailed description of a particular molecular motor.

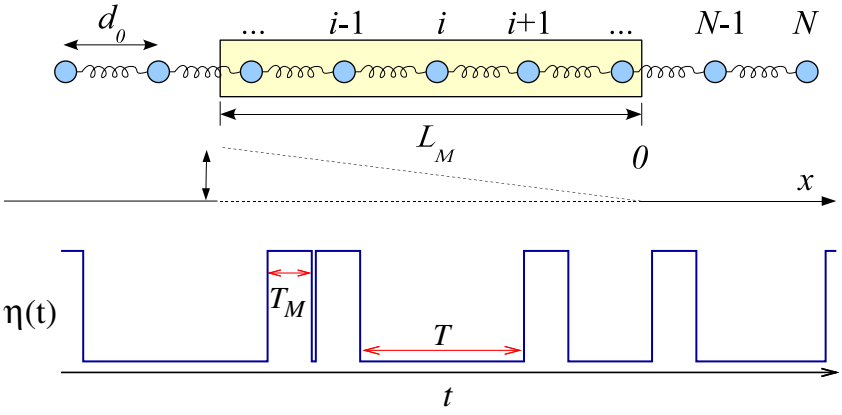

Figure 1. Scheme of the dichotomous pushing force acting on a polymer chain compound by N monomers. T_{M} is the working time of the motor, supposed fixed. T is the mean waiting time in the inactive state. The motor acts on a region of length L_{M}, where the motor action can be expressed by the linear potential $-\eta(t)F_{\mathrm{M}}x$ (with $\eta = 1$ for the active state and $\eta = 0$ for the inactive one), indicated in the middle figure by two dotted lines.

2. The model

The polymer is modelled as a 1D chain of N dimensionless monomers connected by harmonic springs [11]. The total potential energy is $V_{\mathrm{har}} = \frac{k}{2}\sum_{i=1}^{N-1}(x_{i+1} - x_i - d_0)^2$, where k is the elastic constant, x_i the position of the ith particle, and d_0 the equilibrium distance between adjacent monomers. Throughout this paper, $d_0 = 1$ and $k = 1$.

The translocation is helped by the presence of an ATP-activated molecular motor. It has spatial width L_{M} and we set at $x = 0$ its right edge (see figure 1). The motor is characterized by a fixed working time T_{M} which follows the ATP absorption, which, in turn, occurs after a mean waiting time T, depending on the very ATP concentration. In this sense the ATP molecules act on the motor as a shot noise contribution able to switch on its activity. The motor exerts a dichotomous force $F_{\mathrm{M}}\eta(t)$ on the particles inside the motor ($x \in [-L_{\mathrm{M}}, 0]$), where $\eta(t)$ is 1 during the working time and 0 otherwise. As shown in [12], the ATP absorption follows an exponential distribution of waiting times: the probability for an ATP adsorption in a time between t' and $t' + \mathrm{d}t'$ after the last activity is proportional to $\mathrm{e}^{-t'/T}$. Thus, the activation probability of the motor is given by $P_{t'} = 1 - \mathrm{e}^{-t'/T}$ with t' being the motor residence time in its inactive state.

The dynamics of the ith monomer of the chain is described by the following overdamped Langevin equation:

$$\dot{x}_i = -V'_{\mathrm{har}} + F_{\mathrm{M}}\eta_i(t) + \xi_i(t), \tag{1}$$

where the damping (considered the same for all the monomers, which feel the viscosity independently of each other) is included in the normalized time. In the above dimensionless equation, d_0 is taken as the unit of length, the force is expressed in units of kd_0 and the energy is expressed in units of kd_0^2. $\xi_i(t)$ are the Gaussian uncorrelated thermal fluctuations which follow the usual statistical properties $\langle\xi_i(t)\rangle = 0$ and $\langle\xi_i(t)\xi_j(t+\tau)\rangle = 2D\delta_{ij}\delta(\tau)$ with $(i, j = 1 \cdots N)$.

3. Energy supply

The energy used by the motor to provide the driving is given by the ATP hydrolysis. In our model, each ATP hydrolysis just activates the motor for a fixed working time T_M. This description avoids more complex details that are beyond the scope of this paper.

As a consequence of the ATP absorption, the motor changes its conformational state and exerts a mean force F_M during a fixed time $T_M = 1/\nu_0$. After that time, the motor returns to its inactive state. A new force is applied when the next suitable ATP quantity is absorbed. It happens after a mean time $T = 1/\nu$, which follows an exponential distribution of waiting times. That way in our description the activation frequency is proportional to the ATP concentration [13]: $\nu \propto [\mathrm{ATP}]$. The hypothesis that the motor works for a fixed time and that the statistics of the arrival of the ATP molecules happens in an exponential distribution appears realistic in good approximation as clearly shown by different experimental works [9, 10, 12, 14, 15].

With this definition the MM law arises naturally from the model. The motor duty ratio, the fraction of time that it is active, is given by

$$\frac{T_M}{T_M + T} = \frac{\nu}{\nu_0 + \nu} = \frac{[\mathrm{ATP}]}{k_M + [\mathrm{ATP}]}, \tag{2}$$

which is an MM law. The only hypothesis included in the derivation of the last equality is that the motor activation rate ν is proportional to the ATP concentration, $k_M = [\mathrm{ATP}]\nu_0/\nu$ being the Michaelis constant.

The relationship between the mechanical description presented and the MM law is deeper than only the statistical ansatz $\nu \propto [\mathrm{ATP}]$. In the MM enzymatic reaction,

$$E + S \xrightarrow{k_1} Z \xrightarrow{k_2} E + P, \tag{3}$$

the rate k_1 represents the probability of forming the compound Z per unit of time and per unit of S ([ATP]), and k_2 gives the probability of forming the product P per unit of time. In our mechanical and individual case (single motor and single ATP event) Z represents the ATP bound to the motor, which occurs with frequency ν ($\sim k_1[\mathrm{ATP}]$), while P represents the motor action, which is completed within a time $T_M = 1/\nu_0$ ($\nu_0 \sim k_2$). These relationships are in agreement with the definition of the Michaelis constant $k_M = k_2/k_1$.

4. Results

We have numerically solved the Langevin equation (1). We are mainly interested in the behaviour of the translocation time τ and velocity v as a function of the motor activation frequency ν. We will compare our results to some theoretical predictions derived below. For every computed point we performed at least $N_{\mathrm{exp}} = 10\,000$ numerical experiments (for low frequency up to 50 000) using a stochastic Runge–Kutta algorithm with a time step $\mathrm{d}t = 0.01$. The polymer is a compound of N monomers and starts with all the spring at the rest length and the last monomer of the chain at $x_N = 0$, just at the exit of the motor. The noise intensity is fixed at the value $D = 0.01$ and the intensity of the force is $F_M = 0.1$. We have chosen $L_M/d_0 = 5.5$.

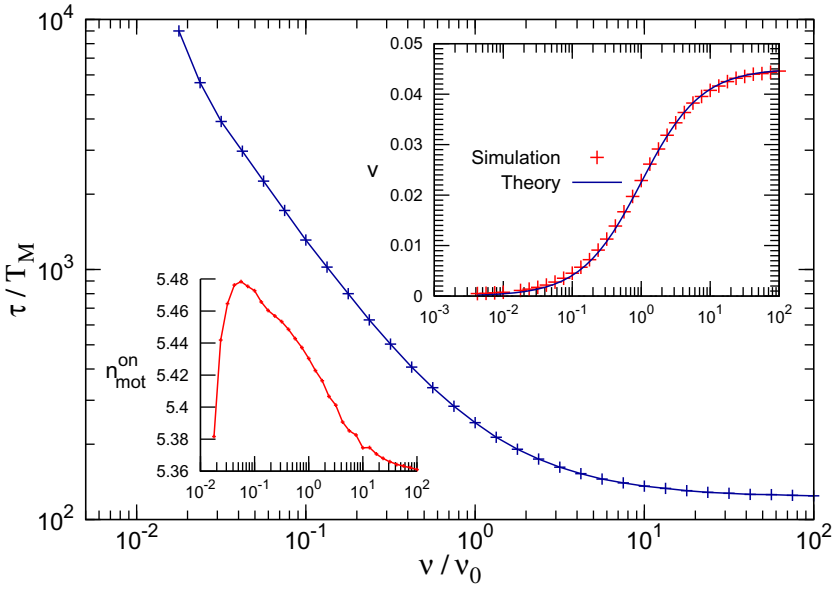

Figure 2. log–log plot of the mean first passage time τ as a function of the mean frequency of the fluctuating force. Top inset: mean velocity, following the MM law given by equation (5). Bottom inset: the mean number of particles inside the motor during its active state. The thermal noise intensity is $D = 0.01$ and $k = 1$.

Polymer translocation. We now study the mean translocation time and velocity of the polymer driven by the motor. With respect to the polymer velocity, by summing up the N terms of equation (1) and averaging in time, we obtain for the centre of mass of the chain the mean velocity v:

$$v = \frac{F_{\mathrm{M}}}{N}\sum_{i=1}^{N}\langle\eta_i(t)\rangle = \frac{F_{\mathrm{M}}}{N}\frac{n_{\mathrm{mot}}^{\mathrm{on}}(\nu)}{1+\nu_0/\nu}. \tag{4}$$

Here $n_{\mathrm{mot}}^{\mathrm{on}}(\nu)$ is the mean number of monomers inside the motor during its activity, a number that is expected to depend weakly on ν. Thus, the mean velocity of the polymer depends on the force felt by the $n_{\mathrm{mot}}^{\mathrm{on}}$ monomers inside the machine which operates for fraction of time $\nu/(\nu_0+\nu)$, and the polymer shows an MM law for the velocity weakly moderated by the function $n_{\mathrm{mot}}^{\mathrm{on}}(\nu)$. Note that this velocity goes to zero as $1/N$ for a large chain as expected for a motor which acts on a small number of monomers and a polymer which moves in a dissipative media.

We also wish to mention that equation (4) is also valid in other interesting situations, for instance, systems with random distributions of T_{M} values with small dispersion around its mean value or the case of a minimum threshold time for the motor activation, which effectively imposes a maximum cutoff frequency in the system (in this case $1/\nu = T_{\mathrm{thres}} + T$).

Figure 2 shows the main observables of the system and their frequency dependence. The translocation time τ is computed as the mean first passage time, i.e. the average over the N_{exp} realizations of the time taken by the centre of mass of the chain to reach the position $x = 0$. It is observed that this time decreases monotonically as ν increases and reaches a limit value for large enough values of ν (T goes to zero and the motor is 'on' most of the time). The relation between translocation velocity v and time τ is not trivial at all, as can be seen in [16] and [17].

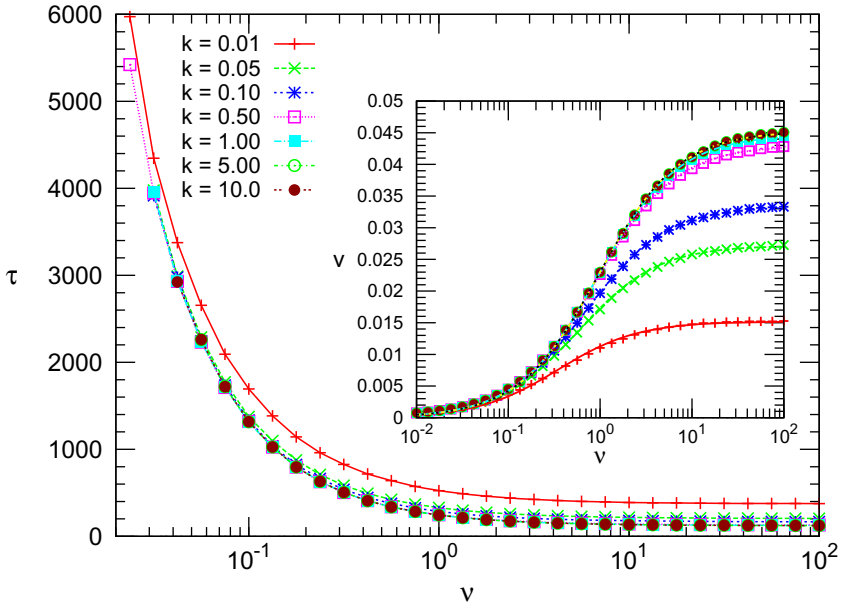

Figure 3. Translocation time and velocity (inset) for different values of the elasticity of the chain k. Lines in the inset show the fit to $v = v^0_{\mathrm{HR}}/(1 + b\nu_0/\nu)$ where $b = 1$ for $k > 0.5$.

The physics of the problem is regulated by the mean number of monomers in the motor during the working time, $n^{\mathrm{on}}_{\mathrm{mot}}$, a number directly related with the elasticity of the chain. As seen in the inset, for the parameters used this number is close to L_{M}/d_0 and does not change importantly in all of the frequency range covered. Thus, as predicted by equation (4) the polymer velocity follows an MM law (see the inset of figure 2):

$$v \simeq v^0_{\mathrm{HR}}/(1 + \nu_0/\nu), \tag{5}$$

with v^0_{HR} being the high-frequency limit ($v^0_{\mathrm{HR}} = 0.0450$ in the plotted case, which is close to $0.0458 = F_{\mathrm{M}} n_{\mathrm{M}}/N$ with $F_{\mathrm{M}} = 0.1$, $N = 12$ and $n_{\mathrm{M}} = L_{\mathrm{M}}/d_0 = 5.5$). Equation (5) allows for a direct experimental fit once the velocity at high ATP concentration (the high rate limit of our system) is measured. With respect to the low-frequency limit, we can see from the equation that v goes to zero as $v \simeq v^0_{\mathrm{HR}}(\nu/\nu_0) \simeq (F_{\mathrm{M}} n_{\mathrm{M}}/N)(\nu/\nu_0)$.

Elastic constant. In order to better understand how the elasticity of the chain acts on the translocation dynamics, we have computed the mean velocity and first passage time (v and τ) for different values of the elastic constant between monomers k (see figure 3). We note that a similar behaviour is observed for the different values considered. As expected, a smaller k gives a lower velocity, the polymer enlarges and the mean number of monomers in the machine diminishes. At low k, $n^{\mathrm{on}}_{\mathrm{mot}}$ changes significantly with ν and v shows deviations with respect to the predictions of equation (5) but can be nicely fitted by a slightly modified law (see the caption of figure 3). For high k ($k > 1$) we reach the rigid chain limit of the system.

Translocation in the presence of a pull force. A set of simulations has been performed by applying a pull force F_{p} on the left extremum of the chain, acting against the motor (see figure 4).

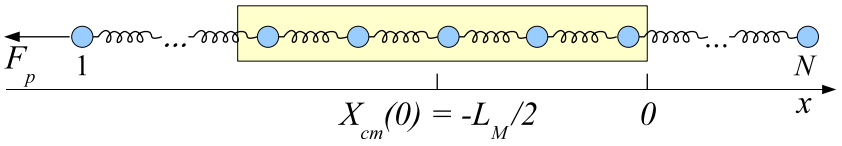

Figure 4. A pull force $F_{\rm p}$ is applied at the chain to measure the stall force of the motor.

The initial condition is set with the polymer centre of mass in the centre of the machine. The velocity of the centre of mass is measured waiting for the exit on the left or on the right of the potential region.

In this case, the mean velocity is given by

$$v = \frac{F_{\rm M}}{N}\,\frac{n^{\rm on}_{\rm mot}(\nu;\,F_{\rm p})}{1+\nu_0/\nu} - \frac{F_{\rm p}}{N}, \tag{6}$$

where the last term $F_{\rm p}/N$ modifies equation (4) by taking into account the presence of an external force acting against the machine. There we emphasize that the presence of a pulling force also modifies the value of $n^{\rm on}_{\rm mot}$ with respect to the unforced value.

Assuming again a weak dependence on ν and $F_{\rm p}$ for $n^{\rm on}_{\rm mot}$, we can rewrite the previous equation as

$$v \simeq \frac{v^{\rm p}_{\rm HR}}{1+\nu_0/\nu} + \frac{v^{\rm p}_{\rm LR}}{1+\nu/\nu_0}, \tag{7}$$

where $v^{\rm p}_{LR} = -F_{\rm p}/N$ is the low-frequency limit of v and $v^{\rm p}_{\rm HR}$ the high-frequency one, $v^{\rm p}_{\rm HR} = (F_{\rm M} n^{\rm on}_{\rm mot;HR} - F_{\rm p})/N$.

Figure 5 (lower inset) shows our numerical results for the polymer velocity in the presence of a pull and it allows for a comparison against the theoretical predictions. As seen in the figure, the polymer mean velocity can be understood in terms of equation (7). Figure 5 shows the excellent agreement between this equation and the numerical calculations once the low and high ATP concentrations (low and high frequency) values are determined. The value of $v^{\rm p}_{\rm HR}$ present in that equation can be evaluated experimentally by using the values of the velocity curves for high ATP concentrations [15]. A rough estimation can also be given by $v^{\rm p}_{\rm HR} \simeq (F_{\rm M} L_{\rm M}/d_0 - F_{\rm p})/N$.

We have also studied the frequency dependence of $n^{\rm on}_{\rm mot}(\nu;\,F_{\rm p})$. As visible in the top inset of figure 5, this quantity depends weakly on ν for all the pulling forces and decreases slightly with $F_{\rm p}$ for all the frequencies. Then the velocity of the polymer shows the expected MM-type behaviour for all the different pull forces used in the calculations ($F_{\rm p} = 0.1, 0.22, 0.34$). We have verified numerically that we can consider $n^{\rm on}_{\rm mot}(\nu,\,F_{\rm p}) \simeq n^{\rm on}_{\rm mot;HR}(F_{\rm p}) \simeq n^{\rm on}_{\rm mot;HR}(0) - a\,F_{\rm p}$. In our case $a \simeq 2.35$ and $n^{\rm on}_{\rm mot;HR}(0) \simeq 5.59$, obtained through a fit procedure of $n^{\rm on}_{\rm mot;HR}(F_{\rm p})$, the high rate values of $n^{\rm on}_{\rm mot}(\nu,\,F_{\rm p})$.

Stall force. We will study now the stall force $F_{\rm stall}$ of the system, which is the value of the pull force $F_{\rm p}$ for which the polymer velocity is zero. In formulae

$$F_{\rm stall} = F_{\rm p}(v=0) = F_{\rm M}\frac{n^{\rm on}_{\rm mot}(\nu,\,F_{\rm p})}{1+\nu_0/\nu} \simeq F_{\rm M}\frac{n^{\rm on}_{\rm mot;HR}(F_{\rm p})}{1+\nu_0/\nu}. \tag{8}$$

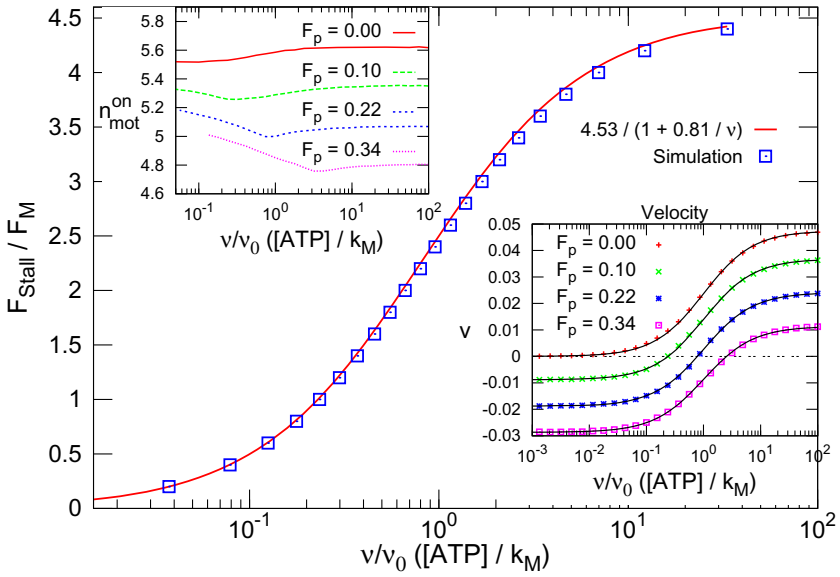

Figure 5. Stall force as a function of the frequency of the dichotomous driving and prediction of equation (10). The insets show, for four values of F_p, $n^{on}_{mot}(\nu)$ (upper inset) and the mean velocity (lower inset) computed (symbols) and predicted (lines) by equation (7).

Here we have used the weak frequency dependence of n^{on}_{mot} as suggested by the inset of figure 5. A simple approximation for $n^{on}_{mot;HR}(F_p)$ is to assume that $n^{on}_{mot;HR} = L_M/d_0$. As discussed above, a more realistic one is to take the linear dependence $n^{on}_{mot;HR}(F_p) \simeq n^{on}_{mot;HR}(0) - aF_p$. Substituting the latter expression into equation (8), we obtain

$$F_p = F_M \frac{n^{on}_{mot;HR}(0)}{1+\nu_0/\nu} - F_M \frac{aF_p}{1+\nu_0/\nu}. \tag{9}$$

By solving with respect to F_p and introducing F_{stall}, we obtain

$$F_{stall} \simeq \frac{F^{HR}_{stall}}{1+b\nu_0/\nu}, \tag{10}$$

where $b = 1/(1+aF_M)$ and $F^{HR}_{stall} \simeq bF_M n^{on}_{mot;HR}(0)$ is the high-frequency stall force.

Figure 5 shows our numerical results for the polymer stall force problem and compares them to our theoretical predictions. We find excellent agreement with the predictions of our equation (10), where $b \simeq 0.81$ and $F^{HR}_{stall} \simeq 0.453$. These numbers results from the values of $a \simeq 2.35$ and $n^{on}_{mot;HR}(0) \simeq 5.59$ obtained above.

In this model, the stall force is *not weakly* dependent on the frequency ν, but changes from 0 to $4.5F_M$ in the range of rate variation of figure 5. Thus an experimental investigation can easily verify the stall force frequency dependence by lowering the ATP concentration in the surroundings of the motor. This way the working model can be verified and tested and also compared with different models[5].

[5] We refer in particular to the outcomes of a similar motor model assisted by both a sinusoidal time dependence [16] and a pure dichotomous driving [17]. Besides the non-trivial behaviours of F_{Stall} as a function of the frequency, a very weak variation of its values is observed there.

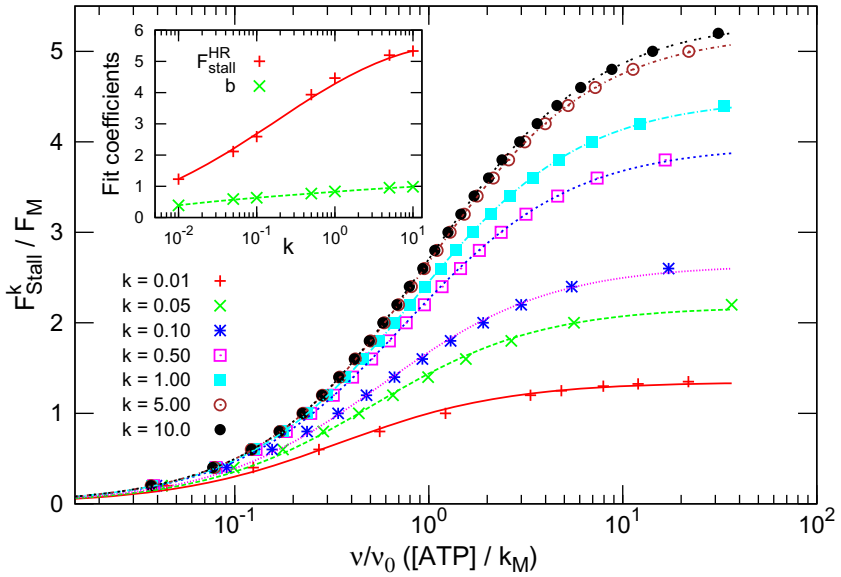

Figure 6. Stall force F^k_{stall} for various values of the elastic parameter k. Lines are the best fit according to equation (10) and the inset shows the values of the fit parameters for different k.

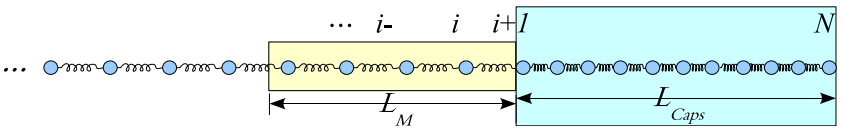

Figure 7. Scheme of the motor pushing the polymer inside the capsid of length L_{Caps}.

Stall force for different k. We have made a number of simulations to study the dependence of the stall force on the elasticity constant k. The results are plotted in figure 6 where the stall force is drawn as a function of the frequency ν for various values of k. We can observe that the stall force increases with k and shows a saturation behaviour at high k (see the curves for $k = 5$ and $k = 10$) similar to that of the velocity (inset of figure 3).

The MM behaviour predicted by equation (10) is observed for all the curves. The inset of the figure shows the behaviour of the coefficients $F^{k,\text{HR}}_{\text{stall}}$ and b of the equation. As expected, the rigid chain (high k) follows an exact MM law, $b = 1$ in equation (10).

Polymer packing. One of the recent most relevant activities in the field is the study of the translocation features in the DNA packing problem driven by molecular motors [12, 14, 15]. One example is the $\phi 29$, a bacteriophage virus that is able to inject its DNA in a bacteria in order to replicate, and then repack it in its capsid. Remarkable experiments [14] have measured the force of the motor as a function of the number of monomers entered in the capsid. The model here depicted is able to qualitatively reproduce the results reported there.

We performed a set of calculations where the chain is pushed into a limited portion of space. Figure 7 shows the scheme of the motor of length L_{M} that pushes the polymer inside a region of length L_{Caps}. The polymer starts with the last monomer on the right at the position

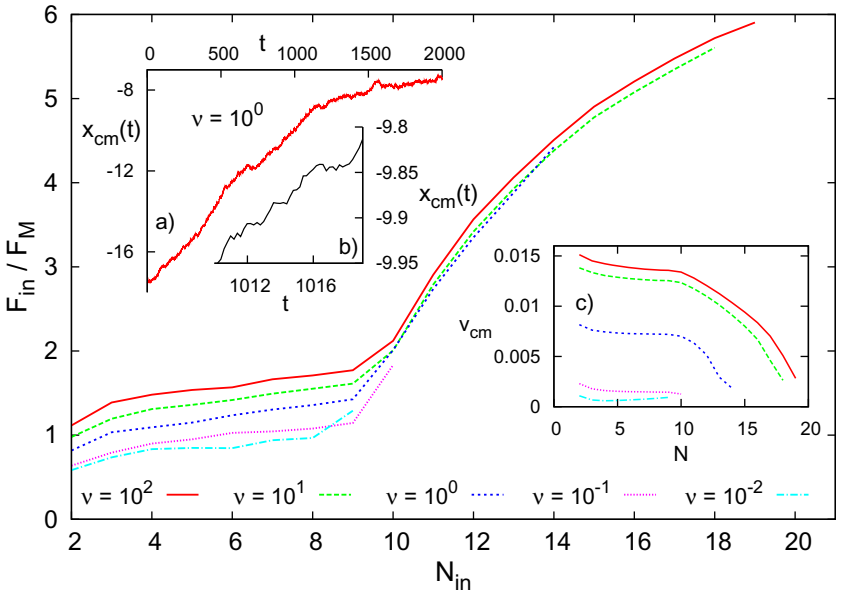

Figure 8. Force on the polymer as a function of the number of monomers entering the capsid (N_{in}). This curve resembles the experimental outcome reported in [14]. The length of the capsid is $L_{\text{Caps}} = 8$ and the number of monomers is $N = 36$. Insets: (a) trajectory of the centre of mass x_{cm} with (b) a small portion showing stops; (c) chain velocity as a function of N_{in}. The activation rate of the motor for the calculations presented in the insets is $\nu = 1$.

$x = 0$. This particle (Nth monomer in the figure) cannot pass the wall on the right. Once there, the polymer begins to compress and the pressure on the particles inside the capsid increases more and more, avoiding in some cases the completion of the translocation process. To consider excluded volume effects and maintain the relative order of the monomers, a repulsive only Lennard–Jones potential has been taken into account in the model: $V_{\text{LJ}}(r) = 4\epsilon[(\frac{\sigma}{r})^{12} - (\frac{\sigma}{r})^{6}]$ for $r \leqslant 2^{1/6}\sigma$ and 0 otherwise. We used $\epsilon = 1$ and $\sigma = 0.1$.

Figure 8 plots F_{in}, the mean force acting on the last monomer entering the capsid, as a function of the total number of monomers entered. The capsid width is $L_{\text{Caps}}/d_0 = 8$ and the chain length is $N = 36$ monomers. It shows that, until the size of the entered polymer is approximately equal to the size of the capsid, the force grows very slowly. Once the last monomer (N) touches the wall of the capsid, the force inside grows rapidly with a saturating trend at a high number of monomers. The inset (c) of the figure plots the polymer mean velocity against the number of monomers in the capsid. We find a behaviour similar to that experimentally observed in [14]. It shows that the model introduced here can depict qualitatively the packing features of the $\phi 29$ motor despite its simplicity.

Biological values. The model we present here is a simplification of both a real polymeric chain and a molecular motor: in the example used here, the DNA and the motor of the $\phi 29$ bacteriophage.

The model is, in principle, adaptable to any translocation process mediated by ATP-based motors, provided that a proper scaling of the measurable quantities can be done. The experimentally possible value of the working time of the motor is $T_{\text{M}} = 10\,\text{ms}$, of the affinity

constant $k_M \simeq 30\,\mu M$ [12] and of the saturation velocity $v_{max} \simeq 103$ DNA base pairs $s^{-1} = 70\,nm\,s^{-1}$ [15]. The saturation velocity sets the v_{HR} value in our model, and the frequency at the MM concentration corresponds to $\nu = \nu_0 = 1/T_M$. Finally, the stall force value found experimentally in the high-frequency limit is $F_{Stall}^{exp} = 57\,pN$ [14]. Using this value we can estimate $F_M \approx 12\,pN$. In the same way the energy consumed per cycle can be obtained for a large ATP concentration as $W = n_{mot}^{on} v_{max} F_M T_M$. With the parameters used, $W \approx 12\,kT_{room}$, which is less than the energy provided by an ATP molecule, i.e. about $20\,kT_{room}$.

5. Discussion

In this paper, we have introduced a simple model for a molecular motor that consumes ATP and produces mechanical work pushing a polymer chain.

Other simple models have been used to describe translocation features of DNA. For instance, in the works of Linke and co-workers, a 1D polymer chain joined together by an FENE potential is studied [18, 19]. The chain moves aided by a flashing extended ratchet potential. By contrast, our potential acts in a limited region of space, which is a more realistic approach to translocation through a pore.

In our paper, we calculate the mean translocation time and the velocity of the polymer as a function of the activation frequency of the motor. The latter shows very good agreement with the experiments and follows a clear MM dependence on the ATP concentration. We see that such MM laws arise in a natural way in the description of the system as a consequence of the kinetics of a machine which remains active for a certain given time. It appears that the *working time average* of the molecular motors that use ATP is actually the origin of the MM law in ATP-motor-assisted dynamics.

We have also studied the behaviour of the polymer in the presence of a pulling force and obtained analytical expressions for the stall force of the system as a function of the ATP concentration. Such expressions, a corrected MM equation, show excellent agreement with our computed results. Finally, the force inside the capsid and the velocity of the chain as a function of the amount of polymer packed have also been evaluated, showing good qualitative agreement with the experiments.

We have studied a 1D model. Polymer translocation experiments are usually performed with the help of optical traps. That way, the polymer (DNA or RNA) is held almost completely stretched out. With respect to the capsid effect, the confinement introduced in the model describes a saturating pressure inside the capsid without taking into account specific geometrical details and polymer recoil effects. For these two reasons the 1D model is a good enough first approach to study the process.

In addition to the fact that technological improvements now allow very precise investigations at the nanoscale, the microscopic working details of the bacteriophage motors are not completely understood. The model is close to one of the two mechanisms proposed recently in [12], where the force acts by means of steric interactions, without chemical bonds with the DNA. Since the DNA packing motor $\phi 29$ is a well-studied motor protein with several intriguing and unexplained features, we have compared our results to experiments with this motor. In general, we found good agreement. However, a detailed model for $\phi 29$ should include many other aspects and is beyond the scope and purpose of this paper. Among these aspects we can mention a precise modelling of the inactive stage, the inclusion of more complex waiting time statistics and the addition of existing structural data.

The results presented here describe the general features of a motor which actuates with a mean force during its cycle. In this sense the qualitative results reported here need some adjustments of the parameters if applied in concrete cases and can be applied to a wide class of ATP-based motors, independently of the inner functioning of the very motor. This paper shows that our model could be a good starting point to develop detailed descriptions of different motors.

Acknowledgments

This work was supported by the Spanish Ministerio de Ciencia e Innovación (MICINN) through project nos. FIS2008-01240 and FIS2011-25167, cofinanced by Fondo Europeo de Desarrollo Regional (FEDER) funds.

References

[1] Zwolak M and di Ventra M 2008 *Rev. Mod. Phys.* **80** 141
[2] Mickler M, Schleiff E and Hugel T 2008 *Chem. Phys. Chem.* **9** 1503
[3] Kasianowicz J J, Brandin E, Branton D and Deamer D W 1996 *Proc. Natl Acad. Sci. USA* **93** 13770
[4] Schneider G F, Kowalczyk S W, Calado V E, Pandraud G, Zandbergen H W, Vandersypen L M K and Dekker C 2010 *Nano Lett.* **10** 3163
[5] Metha D, Rief M, Spudich J A, Smith D A and Simmons R M 1999 *Science* **283** 1689
[6] Starikov E B, Henning D, Yamada H, Gutierrez R, Norden B and Cuniberti G 2009 *Biophys. Rev. Lett.* **4** 209
[7] Gómez-Marín A and Sancho J M 2009 *Eur. Phys. Lett.* **86** 40002
[8] Walter N G 2006 *Nat. Chem. Biol.* **2** 66
[9] English B P, Min W, van Oijen A M, Lee K T , Luo G, Sun H, Cherayil B J, Kou S C and Xie X S 2006 *Nat. Chem. Biol.* **2** 87
[10] Moffit J R, Chemla Y R and Bustamante C 2010 *Proc. Natl Acad. Sci. USA* **107** 15739
[11] Rouse P E J 1953 *J. Chem. Phys.* **21** 1272
[12] Moffitt J R, Chemla Y R, Aathavan K, Grimes S, Jardine P J, Anderson D L and Bustamente C 2009 *Nature* **457** 446
[13] Pérez-Carrasco R and Sancho J M 2010 *Biophys. J.* **98** 2591
[14] Smith D E, Tans S J, Smith S B, Grimes S, Anderson D L and Bustamante C 2001 *Nature* **413** 748
[15] Chemla Y R, Aathavan K, Michaelis J, Grimes S, Jardine P J, Anderson D L and Bustamante C 2005 *Cell* **122** 683
[16] Fiasconaro A, Mazo J J and Falo F 2010 *Phys. Rev.* E **82** 031803
[17] Fiasconaro A, Mazo J J and Falo F *J. Stat. Mech.* (2011) P11002
[18] Downton M T, Zuckermann M J, Craig E M, Plischke M and Linke H 2006 *Phys. Rev.* E **73** 011909
[19] Craig E M, Zuckermann M J and Linke H 2006 *Phys. Rev.* E **73** 051106